1. G Valarmathy[1], 2. N Umapathi[2], 3.Su Suganthi[3], 4. R.Jegadeesan[4]

Sri Sairam Engineering College (1), Jyothishmathi Institute of Technology and Science (2) (4), Sri Sai Ram Institute of Technology(3)
ORCID: (1) 0000-0001-9624-5317, (2) 0000-0002-3639-6794, (3) 0000-0002-7585-8883,(4) 0000-0001-8885-7241

doi:10.15199/48.2024.07.32

An Automated Framework to Segment and Classify Gliomas using Hybrid Shuffled Complex Evolution with Convolutional Neural Network

Abstract*. The infiltrative nature and rapid progression of gliomas have made them the most prevalent as well as aggressive type of brain tumour. In the clinical routine, it is a difficult task to distinguish tumour boundaries from the healthy cells. For brain tumour diagnoses as well as evaluations of the intra operative treatment response, there is extensive utilisation of the Magnetic Resonance Imaging (MRI). With segmentation, infected regions of the brain tissue can be extracted from MRIs. The tumour region's segmentation is a critical task for cancer diagnosis, treatment as well as treatment outcome assessment. The significant architecture named the Convolutional Neural Network (CNN) in deep learning is used. The CNN has shown outstanding improvement in the objects' recognition as well as classification. It has much efficiency in a wide range of problems which deal with machine learning as well as computer vision. Akin to other techniques of deep learning, much difficulty is involved in training the CNN. In this work, proposed a novel meta-heuristic based algorithms have been used for optimizing CNN using Ant Colony Optimization (ACO), hybrid Shuffled Complex Evolution (SCE) with ACO and hybrid SCE with Particle Swarm Optimization (PSO) algorithm. The results show that the proposed method produces better results than existing methods.*

Streszczenie. Naciekowy charakter i szybki postęp glejaków uczyniły je najczęstszym i najbardziej agresywnym rodzajem nowotworu mózgu. W praktyce *klinicznej odróżnienie granic guza od zdrowych komórek jest trudnym zadaniem. W diagnostyce guza mózgu, a także ocenie śródoperacyjnej odpowiedzi na leczenie szeroko wykorzystuje się obrazowanie metodą rezonansu magnetycznego (MRI). Dzięki segmentacji zakażone obszary tkanki mózgowej można wyodrębnić z rezonansu magnetycznego. Segmentacja regionu nowotworowego jest kluczowym zadaniem w diagnostyce nowotworu, jego leczeniu, a także ocenie wyników leczenia. W głębokim uczeniu się wykorzystywana jest znacząca architektura zwana konwolucyjną siecią neuronową (CNN). CNN wykazało wyjątkową poprawę w zakresie rozpoznawania i klasyfikacji obiektów. Ma dużą skuteczność w szerokim zakresie problemów związanych z uczeniem maszynowym i wizją komputerową. Podobnie jak w przypadku innych technik głębokiego uczenia się, szkolenie CNN wiąże się z wieloma trudnościami. W tej pracy zaproponowane nowatorskie algorytmy oparte na metaheurystyce zostały wykorzystane do optymalizacji CNN przy użyciu algorytmu Ant Colony Optimization (ACO), hybrydowej Shuffled Complex Evolution (SCE) z ACO i hybrydowego SCE z algorytmem Particle Swarm Optimization (PSO). Wyniki pokazują, że proponowana metoda daje lepsze wyniki niż metody istniejące.* (***Zautomatyzowany system segmentacji i klasyfikacji glejaków przy użyciu hybrydowej, tasowanej ewolucji złożonej z konwolucyjną siecią neuronową***)

Keywords: Glioma Detection and Segmentation, Magnetic Resonance Imaging (MRI), Gabor Filter, Ant Colony Optimization (ACO), Shuffle Complex Evolution (SCE),Particle Swarm Optimization and Convolutional Neural Network.
Słowa kluczowe: Wykrywanie i segmentacja glejaka, obrazowanie rezonansu magnetycznego (MRI), filtr Gabora, optymalizacja kolonii mrówek (ACO), ewolucja kompleksu losowego (SCE), optymalizacja roju cząstek i konwolucyjna sieć neuronowa

Introduction

Brain tumours are the dominant causes of cancer patient deaths, particularly in children and young people. A report by the American Cancer Society found that, in 2019, the USA had 23,820 new cases of brain cancer. The two major brain tumour types are primary and secondary brain tumour. While the primary type originates in the brain cells, the secondary type develops the spread of malignant cells from other parts to the brain. A commonly occurring primary tumours named Glioma which will affect the brain's glial cells and also will invade the tissues which surround it. The most aggressive as well as common brain tumour type, High-Grade Glioma (HGG) or Glioblastoma (GBM),has a median survival rate of 1-2 years only. On the other hand, Low-Grade Glioma (LGG) like astrocytoma has a slower-growth and has a slightly longer time for survival. Chemotherapy and radiotherapy are some of the recent treatment methods which are utilised for the destruction of tumour cells which cannot be physically resected or for slowing their growth. Hence, for numerous brain tumours, neurosurgery is the preliminary and, in certain cases, the sole course of treatment. Despite that, the brain's nature as well as structure has produced the most cumbersome practice conditions for modern surgical treatment. Furthermore, it is quite challenging for neurosurgeons to differentiate tumour tissue from usual parenchyma only based on visual level [1].

In clinical practice, there is extensively utilisation of the Magnetic Resonance Imaging (MRI) for non-invasive treatment as well as gliomas follow ups. For the purpose of tumour evaluations, there is utilisation of conventional MRI modalities includingT1weighted (T1), enhanced T1-weighted (T1-Gd) with post-contrast, T2weighted modality, and T2-Fluid-Attenuated based Inversion Recovery (FLAIR) image dataset. These Magnetic Resonance Imaging technique produced images are able to offer information about brain tumour's anatomical characteristics. Moreover, additional microvascular, micro structural, and biochemical information is offered by the advanced MRI modalities such as diffusion tensor-weighted, diffusion-weighted, perfusion weighted, MR spectroscopic imaging, and so on [2].

In image processing, the crucial task of image segmentation is done during the processing phase inclusive of low-level images. Partition of homogenous part involved in this task. While brain tumour image segmentation approach is refer for this partition, it will also divide the brain tumour region area. Morphological operations technique and edge detection are some of the various applied methods for image segmentation. It was proved from numerous earlier image segmentation research that higher accuracy outcomes could be offered by the region-based techniques. Nevertheless, the automated brain tumour segmentation was investigated only by few researchers. Watershed edge detection methods followed by image region growth, thresholding, image splitting, merging and analytical morphology are the various applied image segmentation methods used for segmenting the region area [3].

While there have been recent developments in fully automatic as well as semi-automatic algorithms for brain tumour segmentation, this task continues to have numerous opening challenges primarily due to the brain tumours' high

variation in location, regularity, shape, size and heterogeneous appearance (for example, texture, contrast uptake and image uniformity). In addition, there is the inclusion of other potentially complex issues in brain tumour segmentation such as:(1) the Blood-Brain Barrier (BBB) remains integral with LGG cases then the affected part that often not applicable contrast enhancement; hence, LGG's regions may turn out to be blurry or invisible even though the FLAIR sequence offers comparison among the normal and the brain tumour such that there is delineation of the lesion's full extent; (2) contrastingly, in HGG cases, leakage of the gadolinium across the disrupted BBB leads to its entry to the brain tumour's extracellular space and result in hyper intensity on the T1-weighted images. Thus, there will be easy delineation of the necrosis and active tumour regions. However, the HGG often exhibits unclear and irregular boundaries which may also involve discontinuities because of the tumour's aggressive infiltration. This in turn, may cause problems and may lead to poor tumour segmentation; (3) multimodal MRI data is taken into account to detect the visibility of numerous tumour sub-regions as well as types of tumours. Nevertheless, it is quite challenging for co-registration across multiple MRI sequences, particularly when these sequences' acquisition have been done in diverse spatial resolutions; and (4) the general acquisition of generic clinical MRI images is done with much lower inter-slice resolution as well as higher in-plane resolution so as to yield a balance between sufficient image slices for covering the entire tumour volume with good quality cross-sectional views as well as for providing reduced times for scanning. However, this may create the signal-to-noise ratio of in sufficient level as well as effects of asymmetrical half volume have an impact on the accuracy of the final segmentation [4].

Structure tensor eigen values, local histograms, and image textures are the various MRI features which have been adopted in the studies associated with brain tumour segmentation. For pattern recognition in tumour segmentation studies, the frequently used ML methods are the Random Forest (RF) and the Support Vector Machines (SVMs). Deep-learning-based techniques as well as methods enjoy much popularity in brain tumour segmentation research due to its outstanding performance in the fields of image analysis like object detection, semantic segmentation as well as image classification. DL methods are able to accomplish highly advanced performance for automatic brain tumour segmentation through multi-model MRI usage. Being a powerful technique for image recognition as well as prediction, the Convolutional Neural Network (CNN) gets primarily utilised for brain tumour segmentation, classification as well as prediction of patient survival times. Stacked De-Noising Auto-encoders and Convolutional Restricted Boltzman Machine are some of the other deep-learning-based techniques utilised for tumour segmentation, classification as well as prediction. Amongst the various deep learning techniques as well as methods, CNNs have the best performance for image segmentation, classification as well as prediction [5].

Nowadays, certain metaheuristic algorithms have been employed for the optimisation of deep learning, in particular, the CNN. Metaheuristic is a powerful resolution method for challenging optimisation problems, and also has been extensively utilised in almost all areas of research such asscience, engineering, and industrial application. Typically, this method operates on three key objectives, that is, the resolution of huge problems, quicker problem resolution, and the detection of robust algorithms. Furthermore, these methods are easily designable, flexible as well as relative ease for applicability. Majority of the meta-heuristics algorithms are nature-inspired, and are dependent on various principles of phenomena in ethology, physics, and biology [6]. PSO, ACO and Firefly Algorithm (FA) are a few examples of metaheuristic algorithms inspired by ethological phenomena. While Simulated Annealing (SA), Micro-canonical Annealing (MA), and Threshold Accepting method (TA) are examples of metaheuristic algorithms inspired by physical phenomena, Genetic Algorithm (GA), Differential Evolution (DE) and Evolution Strategy (ES)are a few examples of metaheuristic algorithms inspired by biological phenomena.

In this work, proposes the hybrid SCE-ACO and SCE-PSO algorithm for gliomas detection-based MRI. The organization of this paper as follows. Section 2describes the related works in literature. Section 3discussesproposed methods applied in the work. Section 4 discusses experimental results and section 5 concludes the proposed work.

RELATED WORKS

Mzoughi et al., [7] had proposed an effective as well as multi-scale three-dimensional CNN to categorize the glioma tumour into low grade gliomas as well as high-grade gliomas through utilisation of complete volumetric MRI sequence. The proposed architecture would work via small kernels to combine both local and global contextual details to reduce weights with the basis of a layer in the network. In order to overcome the data heterogeneity, proposal was given for a pre-processing technique which had dependence on intensity normalisation as well as the MRI data's adaptive contrast enhancement. Augmentation technique for data was utilised for effective training of the deep 3D-network. With this work, the impact of the proposed pre-processing as well as data augmentation on the classification accuracy could be examined.

Narmatha et al., [8] had devised for the purposes of medical image segmentation as well as classification, the Fuzzy Brain-Storm Optimisation (FBSO) algorithm. This algorithm would combine the fuzzy and Brain-Storm Optimisation (BSO) techniques. While the BSO was primarily focused on the cluster centres and offered these centres the highest priority; akin to just like any other swarm algorithms, it would still get trapped in the local optima. While the fuzzy would carry out various iterations in order to offer an optimal network structure, the BSO would provide better outcomes over other techniques. Dataset's utilisation with the (BRATs 2018), FBSO was found to be less efficient where significantly decreased optimisation algorithm's segmentation duration with precision of94.77%,accuracy of93.85%,sensitivityof 95.77%, and 95.42%F1 score.

Hedyehzadeh et al. [9] had put forward an automated non-invasive estimation technique for the brain tumour's grade with MRI utilisation. Upon completion of pre-processing, the tumour region from the post-processed images then extracted using Fuzzy based segmentation. Extracting the features obtained Matlab software was utilised to extract texture, local inarypattern with fractal based attributes. Afterwards, the Grasshopper Optimisation Algorithm (GOA) was used to optimise the parameters of three distinct methods of classification: Random Forest (RF), K-Nearest Neighbour (KNN), and Support Vector Machine (SVM). Eventually, a performance comparison was done on the three applied classifiers prior to and after the optimisation. When compared with the other classification methods, it was evident that the Random Forest provides better results with 99.09%accuracy.

Saravanan & Thirumurugan [10] utilised optimisation and machine learning techniques to offer high levels of

tumour region segmentation. Initially, edge detection is applied for identifying the edge pixels. Then, this edge detected pixels were applied with the contrast adaptive histogram equalisation method to attain an enhanced brain image. Afterwards, there was the Ridgelet transform's application on this image to obtain the Ridgelet multi-resolution coefficients. Moreover, the Ridgelet transformed coefficients were utilised for the derivation of features, which were then optimised with the Principal Component Analysis (PCA) method. Eventually, the fuzzy system-based classifier was employed for the classification of these optimised features into non-Glioma or Glioma brain images. In comparison with existing classification approach resulted the 97.6%sensitivity, 98.56% specificity,98.73%accuracy,98.85% precision,98.11false positive rate, and 98.185% false negative rate.

Kumar et al., [11] had combined Whale Optimisation algorithms based differential evolution method for the presentation image segmentation technique for brain tumour detection. Moreover, for validation of the proposed hybrid algorithm's efficiency, between-class variance as well as T sall is entropy functions were used for its comparison with certain previously well-known metaheuristic algorithms. For all entropy-based segmentation done on brain MRIs, this proposed hybrid algorithm for image segmentation accomplished much superior results compared to other algorithms.

Devanathan & Venkatachalapathy [12] proposed thresholding with multilevel based segmentation technique and classification approach to diagnosis the brain tumour. At first, the proposed model would enhance the image quality through the execution of pre-processing in three levels. Then, image segmentation was done by the thresholding integration of artificial bee colony algorithm. Later, there was a feasible feature vector set's extraction through utilisation of the feature extractor technique of gray level co-occurrence matrix. In the end, the SVM was used to carry out the classification procedure. With the benchmark Kaggle dataset, a set of simulations were executed. Then, the obtained experimental outcomes were investigated under different aspects. It was demonstrated from the experimental outcomes that the presented model showed an effective diagnostic performance with 97.90%sensitivity, 97.91%specificity, and 97.56%accuracy.

Anaraki et al., [13] had given the proposal for a technique which was on the basis of CNNs as well as the Genetic Algorithm (GA) for non-invasive classification of the diverse Glioma grade by utilising MRI. The existing selection methods for deep neural network architecture are often on the basis of either trial and error or adopting of predefined common architectures. The proposed CNN's structure through GA utilisation. In addition, there is utilisation of an ensemble algorithm on the best GA involved model to minimise prediction error's variance. It was found from a single case study that the three distinct Glioma grades' classification has an accuracy of 90.9%.

METHODOLOGY

The process of feature extraction had resulted in an object's description with regards to the measurable parameters which represent edits relevant attributes, and also could be utilised for classification through setting the object to the class. There is utilisation of image features for the segmentation of colour and texture features, even though the nature of a separate feature which texture image utilises level gray scale whilst colour extracting all the information on the colour space [14]. In 1946, Gabor had introduced one of the most renowned texture descriptors, the Gabor filter. This filter analysed the frequency of considered image domain for feature extraction. Gabor filter was a Gaussian function that underwent modulation by the complex sinusoidal of frequency as well as orientation. This filter operates the domains of spatial and frequency. It could be in a diverse more dimensions. As these filters could offer the finer distinctions of the diverse textures, they were more desirable. The following steps are involved in the analysis of the Gabor filter: get the image's Fourier transform, its multiplication with Gaussian function centred by numerous frequencies by inverse fast fourier transform results. Each Gaussian's selection of the central frequency was critical in ensuring that all image frequencies had been accounted for [15]. This section will provide discussions on the SCE, the ACO-CNN, the SCE-ACO, and the SCE-PSO methods.

3.1 Shuffled Complex Evolution (SCE) Algorithm

The utilized technique Shuffled Complex Evolution-University of Arizona(SCE-UA) is the general-purpose global optimisation method had been proposed for inference of conventional best parameter fixed as well as parameters are underlying with posterior supplies enclosed with individual optimisation run. The objective of the classical SCE-UA algorithm involved to detect the best parameters within the instance space. First, the SCE-UA selects the samples randomly in whole points which are distributed across the bounded parameter space. It will utilise adaptation layer and Downhill Simplex search method for the continuous evolution population towards good decisions in the instance space while continuously surrendering livelihood of boundaries with lesser posterior distribution. Various evolutionary search algorithms [16] are used to observed this genetic drift in which the population's members will drift to individual location in the features space with the mode of $p(\vec{x} \mid f)$.

The SCE algorithm's preliminary proposal was as a method of optimisation for addressing the continuous problems. Nevertheless, numerous problems of optimisation like features election, take place within a features discrete space, which has qualitative dissimilarities between variables as well as between levels. For extension of the SCE algorithm's applicability, there was a binary SCE's development for the resolution of discrete problems. Each complex's position would get encoded by a binary string. Each bit will represent a feature; where a non-selected feature's representation is by the bit value 0, while a selected feature's representation is by the bit value 1. Each position would be a subset of features.

The below steps present the algorithm of SCE-UA [17]:

Step 1 Initialisation: Initialise the selection procedure parameters as follows: q which indicates the number of complexes, np which indicates each complex's number of points, s = np x q, which indicates the size of the population, npq which indicates each sub-complex's number of points, nspl which indicates the number of evolution steps allowed for each complex prior to complex shuffling, minq which indicates required complexes with minimum number when the number of complexity is permitted for decreasing with progression search, maxn which indicates the maximum number of trials allowed prior to the optimisation's termination, k indicates the number of shuffling loops in which the criterion value must modify by pc prior to the optimisation's termination, and pc represents the percent of the criterion value should modify in kth shuffling loops.

Step 2: performance Evaluation:
There is initialisation of an individual population, where $\vec{x}_i$ for i=1,...,s , with randomly generated numbers in accordance with a distribution that is uniform for the n dimensional feature space. The selection of these first individual numbers are inside the user represented bounds, $[x_j^L, x_j^U]$, in which x_j^L will denote the lower boundary constraint while x_j^U will denote the higher region constraint for the values $j = 1,...,n,\ \vec{x} \in F$, wherein s will denote actual size of the population in Equation (1),that is,

$$\vec{x}_i = rnd(x_j^U - x_j^L) + x_j^L \quad i = 1,...,s;\ j = 1,...,n \tag{1}$$

Then, assess the performance with regards to the objective function (OF) value.
Step 3: Sorting the values: Sorting the s considered points in the OF's ascending order in such a way in which first point will indicate and having lowest OF where minimisation issue.

Step 4: Partitioning the points:
There will be division of the population into q complexes, $C^1, C^2, ..., C^q$, where every complex will constitute np points in such a way that the first complex has every q(j−1) + 1 ranked point, the second complex has every q(j−1) + 2ranked point of D, etc., wherein j=1, 2,. . .,np.

Step 5: Evolution: Take nspl evolution steps for each complex's independent evolution. The 2 types of evolution including reflection based evolution and contraction based evolution which follows the Downhill Simplex method's adaptation procedures.

Step 6: Combination of different complexes and population modification: There is combination of the evolved complexes' points to form a single population of samples; sort this population in the criterion value's ascending order; in accordance with the specified procedure in Step 4, re-partition means shuffle the different population of samples into diving the q complexes.

Step 7: Criterion #1: when the number of training trials are greater than tmax. Then, criterion number does not have an improvement in pc×100% in k loops, come to a halt; otherwise, proceed as earlier.

Step 8: Criterion #2: When minq< q, discarding complex which has low rank points, then, set the q values is q−1 and s is np×q, and shift return to step 4. When minq is q, shift backwards to Step 4.

3.2 ACO-CNN

This work as given the proposal for the latest Swarm Intelligence (SI) based Neural Architecture Search (NAS) method. This work will initially concentrate on one of the renowned deep neural architectures, the CNN. The proposed method employs ACO for the discovery of new CNN architectures. For the NAS, the SI is used because of its various feasible traits such as ability to share as well as combine knowledge, scalability, decentralisation, fault tolerance, etc., which would support the management of NAS problems. To be more specific, certain distinct characteristics of the ACO makes it a natural fit for the field of NAS: ACO is best-suited for the resolution of discrete problems that have graphical representations, and also can quickly adapt to the dynamic environment (that is, varying graph). Yet another key factor in its utilisation lies in the fact that there has not been much exploration of the majority of the SI methods within the context of NAS [18].
Akin to the Progressive Neural Architecture Search (PNAS), the Deep Swarm searches for novel architectures in the complexity's ascending order. During the NAS task's commencement, the deep swarm will create the internal graph had input node only. Later, there is generation of a constrained number of ants. Then, 1 at a time, all ants are kept in the input node. After this, individual ant will choose an available node in the CNN's subsequent layer as per Ant Colony System (ACS)choice rule given by the below Equation (2):

$$s = \begin{cases} \arg\max_{u \in J_k(r)} \{[\tau(r,u)].[\eta(r,u)]^\beta\}, & if\ \ q \le q0\ (\text{exp}loitation). \\ S, & otherwise\ (biased\ \ \text{exp}loration), \end{cases} \tag{2}$$

Here, $\tau(r,u)$ will denote amount of pheromone on the edge which extends from node r to node u while $\eta(r,u)$ will denote the associated heuristic value of the edge which extends from node r to node u. Moreover, $J_k(r)$ will denote an available node set which can visit from node r. Number q will be number randomly having uniform distribution over [0….1]. parameters $q_0 \in (0,1]$ and $\beta \in (0, \inf)$ will control the greediness of algorithm as well as heuristic information's relative importance. In the end, S will denote a random variable that was chosen as per the probabilistic distribution defined in the below Equation (3):

$$p_k(r,s) = \begin{cases} \dfrac{[\tau(r,s)].[\eta(r,s)]^\beta}{\sum_{u \in J_k(r)} [\tau(r,u)].[\eta(r,u)]^\beta}, & if\ \ s \in J_k(r). \\ 0, & otherwise. \end{cases} \tag{3}$$

Upon a node's selection, the system will check whether these nodes existed already in the graph in depth selection. When selection for new node that does not exist in the graph, this will get appended with the graph as the previous nodes(that is, node where ant was prior to its selection) neighbour such that the succeeding ants are able to perform the pheromone information's exploitation. After a particular node is picked by an ant, it will also carry out the selection rule which was defined by Equation (2) as well as Equation (3) for selecting that node's attributes(that is, kernel size, and filter size). Upon completion of the selection, there will be the node's addition to the path of the ant. Upon arrival of an ant at the current value or maximum allowed depth, this path will get converted forwarded to neural network structure. This architecture will then undergo assessment. In addition, upon completion of a walk, the ant will carry out ACS local pheromone update (as per Equation (4)) for every edge has utilized further:

$$\tau(r,s) \leftarrow (1-\rho).\tau(r,s) + \rho.\tau_0 \tag{4}$$

Here, parameter ρ will denote the pheromone decay factor while parameter τ_0 will denote the initial pheromone number. local update rule is processed with this number the pheromone values will decay in such a way that other ants will get driven to explore alternate paths. Upon completion of the evaluation by all the ants, there is identification of the best performance ant the ant which was able to find the structure having the better accuracy. Later, the ant will carry

out ACS global pheromone updated to increase the pheromone values for the best path's identified edges as per the below Equation (5):

$$\tau(r,s) \leftarrow (1-\alpha).\tau(r,s) + \alpha.\Delta\tau(r,s) \quad (5)$$

Here,

$$\Delta\tau(r,s) = \begin{cases} C_{gb}, & if \ \ (r,s) \in global\text{-}best\text{-}tour. \\ 0, & otherwise \end{cases} \quad (6)$$

In this equation, parameter α will have a range of (0; 1) and controls the evaporation of the pheromone. C_{gb} will denote global best tour's that means the highest model accuracy cost. Upon increasing current maximum allowed depth of the graph. There will be generation of a new ant population. Till the maximum depth (which is user-specified) is reached, there is this cycle's repetition.

The following are some of the various fascinating outcomes of the ACO's utilization as a search strategy: (1) straightforward implementation of the weight reusability: it will find the graph's lengthiest common sub-path and will use that sub-path's best weights again, (2) there can be the search space's progressive exploration as the ants are adaptable to the dynamic environment (that is, when there is expansion of the graph from depth n to depth n + 1, it will continue to retain the information that has been collected up to a depth of n + 1), and (3) with the utilisation of domain-specific heuristics (Equation (2) and Equation (3)) by the ACO, domain experts can increase the search's speed by easily offering their own expertise.

3.3 SCE-ACO Algorithm

In the SCE-ACO algorithm, a common search space is shared by the multiple ant colonies. Every ant colony will utilise the ACO algorithm for execution of the search activity as well as the pheromone update strategy. Inside the complex, certain elitist individuals are retained by using the elitist strategy. There is utilisation of the strategy named as min-max ant strategy to set each path's concentration of pheromone. There is utilisation of the conventional SCE algorithm as an evolutionary mechanism. The SCE-ACO algorithm's purpose is to exchange information amongst the sub-complexes, and its frequency, content, and strategy after the execution of certain iterations. These have a direct relation to the SCE-ACO algorithm's efficiency as well as solution quality [19].Description of the various steps involved in the SCE-ACO algorithm are given as below.

Step 1. There is division of the ant colony into many sub-complexes within a common search space, where every sub-complex will execute the search activity as well as the pheromone update strategy. When there is division of multi objective optimisation issue into various sub-optimisation issues, every sub optimisation issue will correspond to a single sub-complex.

Step 2. There is initialisation of SCE-ACO algorithm's parameters: α and β of the control parameters, m is the ant size, ρ is the pheromone trial evaporation rate, T_{max}, is the maximum number of iterations and the t = 0 is iteration algebraic counter. The initialised values of ants, the parameters will get by stored by every ant as $Ant_k^{(t)}(\beta_k, \rho_k, q_k)$.

Step 3:Evaluate value of fitness for every individual in every sub-complex, and determining the outcome will whether fulfil the end condition. When the end condition is fulfilled by results, then this outcome will be given as the output. Else, continue to the next step.

Step 4:In accordance with the improved pheromone updating Equations (4) to (6), there is a pheromone update for each individual.

Step 5. In every sub-complex, certain elitist individuals will get retained with the elitist strategy's utilisation. There is evolution of the other ants for a new complex's generation.

Step 6. Every sub-complex will pick the current optimal individual, and this choice will get utilised to yield a whole solution with another sub-complex's individual for completion of the interaction of information amongst these sub-complexes.

Step 7. Every path's concentration of pheromone is set using the min-max ant strategy, wherein every path's concentration of pheromone is constrained within $[\tau_{\min}, \tau_{\max}]$ range. The value of $\tau_{\max}$ is able for bypass the pheromone quantity of one path than concentration is greater than the other path for prevention of the concentration of all the pheromones on the same path. In addition, $\tau_{\min}$ value is able to efficiently prevent the SCE-ACO algorithm's stagnation.

Step 8. Determine the fulfilment of the maximum number of iterations. If there has been a fulfilment of the maximum iteration number, then there will be an output of the result. Otherwise, shift backwards to Step 3.

3.4 Proposed SCE-PSO CNN Algorithm

In 1995, Kennedy and Eberhart had initially proposed a nature-influenced meta-heuristic known as the PSO. The bird flocks' behaviour is inspired the PSO will control the particles' search for solutions that are globally optimal. In this algorithm, there is random diffusion of the particles are population of across the search space. The assumption is that these particles fly inside the search space. Every particle will have a velocity as well as a position that is iteratively updated on the basis of personal as well as social experiences. Every particle's local memory will store the best so far achieved experience. Furthermore, the global memory will store the best solution found so far. However, the local memory as well as the global memory are constrained in size to one. The particle's personal experience gets represented as the local memory while the swarm's social experience gets represented as the global memory. Randomized correction coefficients are used to maintain a balance between the effects of both personal as well as social experiences. Minimization of the distance between the particle as well as the best personal and social known locations is the operating principle of the process of velocity update. Since the PSO enjoys much ease in implementation, it has been successfully deployed in numerous real-world applications [20].

Every particle in the standard PSO gets treated as a probable solution to the problem of numerical optimisation in a D dimensional space. In this search space, there is assignation of a position as well as a velocity to each particle. $x_i = (x_{i1}, x_{i2}, ..., x_{iD})$ will represent each particle's position while $v_i = (v_{i1}, v_{i2}, ..., v_{iD})$ will represent each particle's velocity. While all particles have their own local memory (p Best) to retain the best position experienced by the particle so far, there is also a globally shared memory (g Best) which will retain the best global position found so far. The below the equations (7 & 8) are used by this information to contribute towards every particle's flying velocity:

(7) $v_i = v_i + \varphi_1 \times rand \times (pBest_i - x_i) + \varphi_2 \times rand \times (gBest_i - x_i)$

(8) $x_i = x_i + v_i$

In these equations, φ_1 and φ_2 are constants which determine the relative influences of the personal as well as the social experiences. The approach's performance can be increased through definition of the velocity component 'supper bound. Equation 8will offer an update of the particle position.

In the standard PSO, guidance of the swarm is carried out by the g best model, that is, the best solution found so far by the entire swarm. Lately, numerous investigations have been done on various neighbourhood topologies for the PSO that utilises the l best model, that is, every particle's best current performance of its neighbours for replacement of the entire swarm's best previous ones. This work has proposed the algorithm SCE-PSO with CNN to utilise the particle's so far best found value of the function for definition of the relations of the neighbourhood. Akin to the l best model, this proposed algorithm will only consider a portion of the swarm to update a particle's velocity. In accordance with the individuals' fitness development, there is a constant change of the algorithm's neighbourhoods [21].

Step 1: Initialisation. Pick$p \geq 1, m \geq 1$, in which, the number of complexes will be denoted as *p*, and each complex's number of points will be denoted as *m*. Evaluate the sample size *s* = *pm*. In the feasible space, the sample*s* has points $X_1, ..., X_s$. At each point X_i, there is evaluation of the function value,f_i.

Step 2: Rank. Sort the points in the function value's increasing order. Use the array $E = \{X_i, f_i, i = 1, ..., s\}$ to store these points.

Step 3: Partition. Divide the array *E* into *p* complexes $A^1, A^2, ..., A^p$, wherein every complex will consist of points *m* and will be: $A^k = \{X_j^k, f_j^k \mid X_j^k = X_{k+p(j-1)}, f_j^k = f_{k+p(j-1)}, j = 1, ..., m\}$.

Step 4: Evolution. Separately use the PSO to evolve each complex A^k.

Step 4.1: Initialisation. Pick *q* and *T*, in which *q* will denote the PSO's population size, and *T* will denote the maximal iterated generation.

Step 4.2: Selection. For a sub-swarm's construction, in accordance with the values of the function, pick *q* distinct points, $Y_1^k, ..., Y_q^k$ from A^k. It is the better points in A^k which have more selection probability. These points can be stored in $F^k = \{Y_i^k, V_i^k, u_i^k, i = 1, ..., q\}$, in which V_i^k will denote the velocity for particle Y_i^k ,and u_i^k will denote the associated value of the function. Identify the position of the best individual of the complex G^k as well as the best previously visited position of each particle P_i^k.

Step 4.3: Comparison. Comparison is drawn between the function valuesof each particle Y_i^k and P_i^k. $P_i^k = Y_i^k$ when Y_i^k is found to be better than P_i^k, then. Comparison is drawn between the function values of each particle Y_i^k and G^k. $Y_i^k = G^k$ when Y_i^k is found to be better than G^k.

Step 4.4: Renewal. Renew each particle's position as well as velocity in accordance with the formulations (7& 8).

Step 4.5: Iteration. Repeat **Step 4.3** and **Step 4.4** *T* number of times, in which *T* will denote a user-specified parameter that determines how quickly each complex must evolve.

Step 5: Shuffling of the complexes. Replace $A^1, A^2, ..., A^p$ into *E*. Sort *E* in the increasing order of function value.

Step 6: Check the convergence. If there is fulfillment of the convergence criteria, then come to a halt. Otherwise, shift backwards to **Step 4**.

The SCE-PSO will incorporate the PSO's strengths, the competitive evolution as well as the complex shuffling concept. It will significantly boost the survivability through the sharing of information which has been independently acquired by each complex. In the SCE-PSO, every member of a complex is a potential parent capable of participating in the evolution process. A selected sub-swarm from the complex is akin to a pair of parents. For guaranteeing a competitive process of evolution, it is essential that, for contribution to the offspring generation, the better parents have a higher probability that the worse parents. In the end, every new offspring will replace the current sub-swarm's worst point instead of that of the whole population. This will ensure that process prior to being discarded or replaced. Hence, there is no ignorance of any information contained in the sample.

4 RESULTS AND DISCUSSION

For the experiment, 182 normal and 47 glioma images are considered. In this section, the ACO-CNN, SCE-ACO CNN and SCE-PSO CNN methods are used. The table 1 shows the summary of results. The classification accuracy, precision, recall, and f measure as shown in figures 1 to 4.

Table 1 Summary of Results

	ACO-CNN	SCE-ACO CNN	SCE-PSO CNN
Classification accuracy	89.52	93.01	95.2
Precision for Non-Gliomas	0.9389	0.9611	0.9777
Precision for Gliomas	0.7347	0.8163	0.86
Recall for Non-Gliomas	0.9286	0.9505	0.9615
Recall for Gliomas	0.766	0.8511	0.9149
F-Measure for Non-Gliomas	0.9337	0.9558	0.9695
F-Measure for Gliomas	0.75	0.8333	0.8866

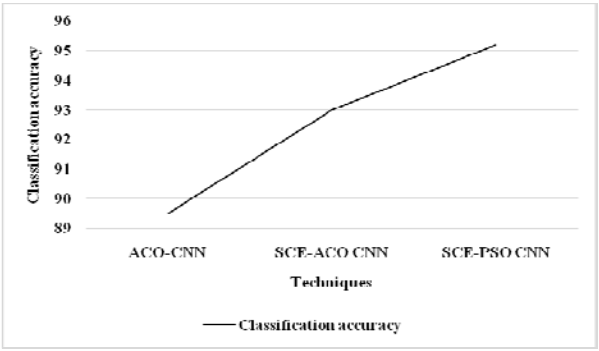

Fig. 1 Classification Accuracy for SCE-PSO CNN

From the figure 1, it can be observed that the SCE-PSO CNN has higher classification accuracy by 6.15% for ACO-CNN and by 2.33% for SCE-ACO CNN respectively.

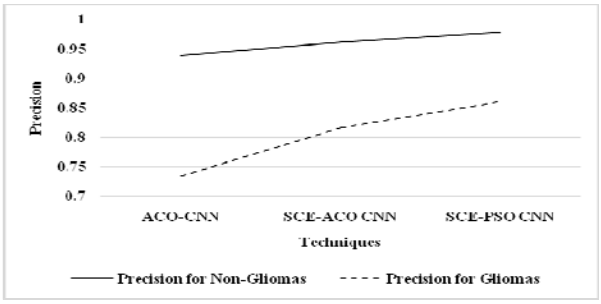

Fig. 2Precision for SCE-PSO CNN

From the figure 2, it can be observed that the SCE-PSO CNN has higher precision for non-gliomas by 4.05% for ACO-CNN and by 1.71% for SCE-ACO CNN respectively. The SCE-PSO CNN has higher precision for gliomas by 15.71% for ACO-CNN and by 5.21% for SCE-ACO CNN respectively.

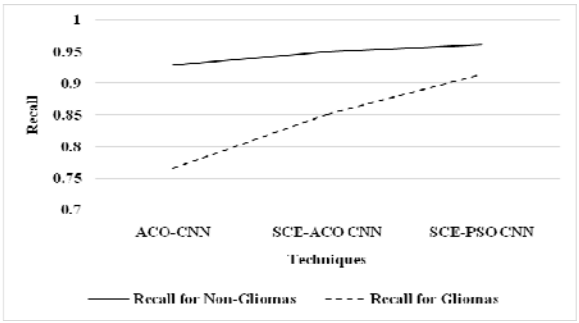

Fig. 3 Recall for SCE-PSO CNN

From the figure 3, it can be observed that the SCE-PSO CNN has higher recall for non-gliomas by 3.48% for ACO-CNN and by 1.15% for SCE-ACO CNN respectively. The SCE-PSO CNN has higher recall for gliomas by 17.72% for ACO-CNN and by 7.22% for SCE-ACO CNN respectively.

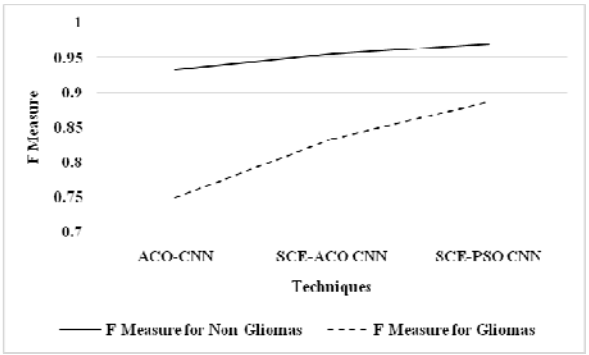

Fig. 4 Measure for SCE-PSO CNN

From the figure 4, it can be observed that the SCE-PSO CNN has higher f measure for non-gliomas by 3.76% for ACO-CNN and by 1.42% for SCE-ACO CNN respectively. The SCE-PSO CNN has higher f measure for gliomas by 16.69% for ACO-CNN and by 6.19% for SCE-ACO CNN respectively.

5 onclusion

Glioma grading has a critical role in the determination of the treatment plan as well as the prognosis prediction. There has been the development of efficient brain tumour grading methods on conventional MRI images which are based on deep CNNs. This work has presented the ACO-CNN which will produce an ant population that utilises the pheromone information in the collective search for the best neural architecture. In addition, this method will ensure a balance between the exploitation and the exploration through utilisation of local as well as global pheromone update rules. The SCE-ACO algorithm will enhance the pheromone update formula as well as restrict the pheromone's update range for realisation of the pheromone's adaptive update. There is division of the multi-objective optimisation problem into various sub-complexes with a corresponding population that will execute the search activity as well as the pheromone update strategy. In this work SCE-PSO algorithm is proposed, a population of points is sampled randomly in the feasible space. Then the population is partitioned into several complexes, which is made to evolve based on PSO. Results show that the SCE-PSO CNN has higher classification accuracy by 6.15% for ACO-CNN and by 2.33% for SCE-ACO CNN respectively.

Equations

For equations it is recommended to use standard equation editor existing in Word editor (usually it is Math Type editor). The equation editor is defined as follows: font Times New Roman italic, matrix bold, for letters font 10, for index 8, for symbol 12. For example, typical equation should be as:

$$J = \sum_{0}^{\infty} A^2 \sin \omega t + \int_{0}^{\infty} \sqrt{B_1^2 + C_2^2} + \frac{4\pi}{\mu_0} \int_V \frac{J \times r}{r^3} dv$$

where: J – current density, r – distance, A,B,C – coefficients.

Insert the equation number on the left side (it seems as strange, but it is old tradition of our journal), between the text and the equation please leave the distance of 6 points. It is not accepted insertion of the equations into tables.

The new versions of Word offer the equation editor not compatible with Math Type - thus after conversion to older version the equation is a very bed quality "bitmap". The solution is to use original Math Type software.

If the figure is as wide as the whole page we can insert two sections lines and between them change the one-column style - as it is presented in Fig. 2.

Please do not insert the figures into the tables (with an exception of special case where we would like to order several sub-figures into one figure).

If there are problems with electronic version of the figures it is recommended to deliver the article with supplemented "hard copies" of the figures. This means that also a "printed version" of the figures should be included for eventual scanning. But of course scanned figure is not as good quality as original one.

It is possible to print figures in the colour version, but Authors should take into account that colour page is much more expensive than black/white and moderation in applying of the colour is advisable.

REFERENCES

[1]. Zeineldin, R. A., Karar, M. E., Coburger, J., Wirtz, C. R., & Burgert, O. (2020). DeepSeg: deep neural network framework for automatic brain tumor segmentation using magnetic resonance FLAIR images. *International journal of computer assisted radiology and surgery*, 15(6), 909-920.

[2]. Zhuge, Y., Ning, H., Mathen, P., Cheng, J. Y., Krauze, A. V., Camphausen, K., & Miller, R. W. (2020). Automated glioma grading on conventional MRI images using deep convolutional neural networks. *Medical physics*, 47(7), 3044-3053.

[3]. Zaihani, N. H. I. M., Roslan, R., Ibrahim, Z., & Samah, K. A. F. A. (2020). Automated segmentation and detection of T1-weighted magnetic resonance imaging brain images of glioma brain tumor. *Bulletin of Electrical Engineering and Informatics*, 9(3), 1032-1037.

[4]. Dong, H., Yang, G., Liu, F., Mo, Y., & Guo, Y. (2017, July). Automatic brain tumor detection and segmentation using u-net based fully convolutional networks. *In annual conference on medical image understanding and analysis* (pp. 506-517). Springer, Cham.

[5]. Nadeem, M. W., Ghamdi, M. A. A., Hussain, M., Khan, M. A., Khan, K. M., Almotiri, S. H., & Butt, S. A. (2020). Brain tumor analysis empowered with deep learning: A review, taxonomy, and future challenges. *Brain sciences*, 10(2), 118.

[6]. Ayumi, V., Rere, L. R., Fanany, M. I., & Arymurthy, A. M. (2016, October). Optimization of convolutional neural network using microcanonical annealing algorithm. *In 2016 International Conference on Advanced Computer Science and Information Systems (ICACSIS)* (pp. 506-511). IEEE.

[7]. Mzoughi, H., Njeh, I., Wali, A., Slima, M. B., Ben Hamida, A., Mhiri, C., & Mahfoudhe, K. B. (2020). Deep multi-scale 3D convolutional neural network (CNN) for MRI gliomas brain tumor classification. *Journal of Digital Imaging*, 33, 903-915.

[8]. Narmatha, C., Eljack, S. M., Tuka, A. A. R. M., Mani murugan, S., & Mustafa, M. (2020). A hybrid fuzzy brain-storm optimization algorithm for the classification of brain tumor MRI images. *Journal of Ambient Intelligence and Humanized Computing,* 1-9.

[9]. Hedyehzadeh, M., Maghooli, K., & Momen Gharibvand, M. (2021). Glioma grade detection using grasshopper optimization algorithm-optimized machine learning methods: The Cancer Imaging Archive study. *International Journal of Imaging Systems and Technology*.

[10]. Saravanan, S., & Thirumurugan, P. (2020). Performance Analysis of Glioma Brain Tumor Segmentation Using Ridgelet Transform and Co-Active Adaptive Neuro Fuzzy Expert System Methodology. *Journal of Medical Imaging and Health Informatics,* 10(11), 2642-2648.

[11]. Kumar, S., Vig, G., Varshney, S., & Bansal, P. (2020). Brain Tumor Detection Based on Multilevel 2D Histogram Image Segmentation Using DEWO Optimization Algorithm. *International Journal of E-Health and Medical Communications (IJEHMC),* 11(3), 71-85.

[12]. Devanathan, B., & Venkatachalapathy, K. (2020, November). An Optimal Multilevel Thresholding based Segmentation and Classification Model for Brain Tumor Diagnosis. *In 2020 4th International Conference on Electronics, Communication and Aerospace Technology (ICECA)* (pp. 1133-1138). IEEE.

[13]. Anaraki, A. K., Ayati, M., & Kazemi, F. (2019). Magnetic resonance imaging-based brain tumor grades classification and grading via convolutional neural networks and genetic algorithms. *biocybernetics and biomedical engineering*, 39(1), 63-74.

[14]. Wicaksono, Y., Wahono, R. S., & Suhartono, V. (2015). Color and texture feature extraction using gabor filter-local binary patterns for image segmentation with fuzzy C-means. *Journal of Intelligent Systems,* 1(1), 15-21.

[15]. Roslan, R., & Jamil, N. (2012, December). Texture feature extraction using 2-D Gabor Filters. *In 2012 International Symposium on Computer Applications and Industrial Electronics (ISCAIE)* (pp. 173-178). IEEE.

[16]. Mariani, V. C., Luvizotto, L. G. J., Guerra, F. A., & dos Santos Coelho, L. (2011). A hybrid shuffled complex evolution approach based on differential evolution for unconstrained optimization. *Applied Mathematics and Computation*, 217(12), 5822-5829.

[17]. Mariani, V. C., & dos Santos Coelho, L. (2011). A hybrid shuffled complex evolution approach with pattern search for unconstrained optimization. *Mathematics and Computers in Simulation,* 81(9), 1901-1909.

[18]. Byla, E., & Pang, W. (2019, September). Deep swarm: Optimising convolutional neural networks using swarm intelligence. *In UK Workshop on Computational Intelligence* (pp. 119-130). Springer, Cham.

[19]. Zhao, H., Gao, W., Deng, W., & Sun, M. (2018). Study on an adaptive co-evolutionary aco algorithm for complex optimization problems. *Symmetry*, 10(4), 104.

[20]. Asta, S., & Uyar, A. S. (2012). A Novel Particle Swarm Optimization Algorithm. *Computer & Informatics Faculty Istanbul Technical University*, Istanbul, Turkey.

[21]. Yan, J., Tiesong, H., Chongchao, H., Xianing, W., & Faling, G. (2007, April). A shuffled complex evolution of particle swarm optimization algorithm. *In International conference on adaptive and natural computing algorithms* (pp. 341-349). Springer, Berlin, Heidelberg.

[22]. Suganthi, S.; Umapathi, N.; Mahdal, M.; Ramachandran, M. Multi Swarm Optimization Based Clustering with Tabu Search in Wireless Sensor Network. *Sensors 2022*, 22, 1736. https://doi.org/10.3390/s22051736,

[23]. N.Umapathi., N.Ramaraj., (2016) Wireless adhoc telemedicine system: proving networking performance for multimedia data. *Journal of medical imaging and health informatics* 6(8), 1944-1948. DOI 10.1166/jmihi.2016.1954